Atmospheric Research 270 (2022) 106081

Contents lists available at ScienceDirect

Atmospheric Research

journal homepage: www.elsevier.com/locate/atmosres

An initial assessment of the distribution of total Flash Rate Density (FRD) in Brazil from GOES-16 Geostationary Lightning Mapper (GLM) observations

Paula S.S. Oda [a,b,*], Diego P. Enoré [c], Enrique V. Mattos [a], Weber A. Gonçalves [d], Rachel I. Albrecht [e]

[a] Natural Resource Institute, Federal University of Itajubá (UNIFEI), Itajubá, Minas Gerais, 37501-151, Brazil
[b] Post Graduate Program in Environmental and Hydrological Studies, Federal University of Itajubá (UNIFEI), Itajubá, Minas Gerais, 37501-151, Brazil
[c] Center for Weather Forecasting and Climate Studies (CPTEC), National Institute for Space Research, Cachoeira Paulista, São Paulo, 12630-000, Brazil
[d] Department of Atmospheric and Climatic Science, Federal University of Rio Grande do Norte (UFRN), Natal, Rio Grande do Norte, 59078-970, Brazil
[e] Department of Atmospheric Sciences, Astronomy Institute, Atmospheric and Geophysical Sciences, University of São Paulo (USP), São Paulo, São Paulo, 05508-090, Brazil

ARTICLE INFO

Keywords:
GOES-16
Lightning activity
Hotspots
Monthly cycle
Diurnal cycle

ABSTRACT

Brazil is one of the regions in the world where lightning most occurs. With the launch of the Geostationary Environmental Operational Satellite – 16 (GOES-16), it was possible, for the first time, to carry out an almost uniform resolution mapping, in near real time, of total lightning with a field of view that covers most of the western hemisphere. The objective of this study was to evaluate the initial spatio-temporal distribution of the Total Lightning Flash Rate Density (FRD) for all of Brazil, and to determine lightning hotspots in cities in five regions, the South, the Southeast, the Midwest, the Northeast, and the North. Total lightning flash data from the Geostationary Lightning Mapper (GLM) sensor on board the GOES-16 were evaluated for a three-years period (from 2018 to 2020). The greatest FRD (about 30 fl km^{-2} season^{-1}) occurred during the hot season (between spring and summer), mostly in the late afternoon (12–18 Local Hour, LH), in the northwest-southeastern portion of the country (AM, PA, MT, GO and TO), in the southeastern of RJ and closer to the Brazil-Argentina border (MS, PR, SC and RS). The lowest FRD values were observed along coastal regions, extending from the north of RJ to AP, and for the north of RO and PA. São Félix do Xingu city in Pará came in first (131 fl km^{-2} year^{-1}) in the national ranking for lightning hotspots, showing well-defined monthly and daytime cycles with maximums at 14 LH.

1. Introduction

Lightning is produced by storm clouds that typically produce severe weather events like hail, intense rain, strong winds, and tornadoes (Williams et al., 1999; Schultz et al., 2011). These events can cause significant damage to many sectors of society, and in extreme cases, can result in deaths among both people and animals. In Brazil about 132 people per year are killed in lightning strikes (Cardoso et al., 2014). Due to Brazil's vast land area and proximity to the equator, it has some of the highest occurrences of lightning in the world (Pinto Jr. and Pinto, 2000; Christian et al., 2003; Cardoso et al., 2014; Albrecht et al., 2016a). Evaluating the spatial and temporal distribution of lightning allows researchers to map regions more vulnerable to lightning strikes and to generate subsidies for producing more effective and regionalized short-term forecasting tools.

Lightning occurs due to the accumulation of electrical charges inside a storm cloud. The accumulation of electrical charges is the result of collisions between small ice crystals and graupel (soft hail), in the presence of super-cooled liquid water in the updraft regions (Reynolds et al., 1957). The lightning flashes are divided into the following categories, intracloud lightning (IC), inter-cloud lightning, cloud-to-ground lightning (CG), ground-to-cloud lightning (GC), and cloud-air lightning (CA) (Ogawa, 1995). However, CG lightning is the most harmful to humans and to various sectors of the economy. For this reason, it is the most studied type of lightning (Kitagawa and Brook, 1960; Kitagawa et al., 1962; Fuquay, 1982; Macgorman and Burgess, 1994).

The first lightning records were recorded by human observers at surface weather stations (Brooks, 1925). In Brazil, the first record was

* Corresponding author at: Federal University of Itajubá (UNIFEI), Natural Resource Institute (IRN), Avenida BPS, 1303, Minas Gerais, MG 37501-151, Brazil.
E-mail address: sayeko@unifei.edu.br (P.S.S. Oda).

https://doi.org/10.1016/j.atmosres.2022.106081
Received 6 September 2021; Received in revised form 24 January 2022; Accepted 8 February 2022
Available online 12 February 2022
0169-8095/© 2022 Elsevier B.V. All rights reserved.

made by German naturalist Georg Marcgrave, and by Dutch naturalist Guilherme Piso, in 1640, in Recife, as cited by *Historia Naturalis Brasiliae* (Sant'anna Neto, 2006). With advances in technology, researchers could improve lightning detection techniques using networks of electromagnetic sensors to monitor surface lightning. Besides recording when lightning flashes, these networks can also estimate the intensity of CG and IC lightning and where they strike (Orville et al., 1983; Cummins et al., 1998). Brazil currently operates six Lightning Location Systems (LLS): i) Brazilian Lightning Detection Network (BrasilDAT) (Naccarato and Pinto, 2012), ii) National Integrated Atmospheric Discharge Detection Network (RINDAT) (Bourscheidt et al., 2012), iii) Sferics Timing and Ranging Network (STARNET) (Morales Rodriguez et al., 2015; Morales Rodriguez, 2019), iv) Lightning Network (LINET) (Höller et al., 2009), v) Global Lightning Dataset (GLD360) (Said et al., 2013) and vi) Worldwide Lightning Location Network (WWLLN) (Lay et al., 2004). Despite providing the location of lightning flashes, these LLS offer limited non-homogeneous spatial coverage, or relatively lower detection efficiencies. Thus, they do not offer information on remote or difficult to access regions.

In the 1960s, the first estimates of total lightning flashes (i.e., IC + CG) were made from space (Albrecht et al., 2014). In 1995, the National Aeronautics and Space Administration (NASA) launched the first on board satellite instrument specifically designed to detect lightning. It was called the Optical Transient Detector (OTD), on board the MicroLab-1 communications satellite (Christian et al., 2003). In 1997, the Lightning Imaging Sensor (LIS) was launched by NASA in conjunction with the Japanese Aerospace Exploration Agency (JAXA) on board the Tropical Rainfall Measuring Mission (TRMM) (Boccippio et al., 2000; Cecil et al., 2014; Albrecht et al., 2016a). More recently, in November 2016, NASA, in conjunction with the National Oceanic and Atmospheric Administration (NOAA), launched the Geostationary Operational Environmental Satellite - 16 (GOES-16) extending lightning observations from space beyond the OTD (1995–2000) and the LIS (1997–2015) mission (Goodman et al., 2013; Rudlosky et al., 2019; Zhang and Cummins, 2020; Murphy and Said, 2020). This satellite has a Geostationary Lightning Mapper (GLM) sensor on board, which can map lightning, providing information based on real events (illuminating single pixels, minimum units), groups (adjacent events), and flashes (sequence of one or more groups) (Mach et al., 2007; Goodman et al., 2012).

Christian et al. (2003), analyzed the spatial and temporal distribution of lightning around the globe using 5 years of data (May 1995 to March 2000) from the OTD sensor. The authors documented an average global annual rate of 44 ± 5 lightning flashes per second. Lightning occurrence peaked in the Northern and Southern Hemispheres in their respective summer periods. Additionally, Cecil et al. (2014), combined data from the OTD and LIS sensors with a spatial resolution of 0.5°. The authors documented a minimum global rate of 35 lightning flashes per second in February, and a maximum rate of 60 lightning flashes per second in August. Recently, Albrecht et al. (2016a), compiled 17 years of data from the LIS sensor on board the TRMM satellite with a spatial resolution of 0.1° and found a high (20 to 40 fl km^{-2} year^{-1}) flash rate density for South America, with the most extreme events in northern Argentina, extending to Paraguay, and Brazil. Specifically for Brazil, the authors documented a maximum (20–30 fl km^{-2} year^{-1}) rate of lightning flashes in the northwest of Rio Grande do Sul state and in the west of Santa Catarina. Furthermore, high rates of lightning occurrence were found for the region where the South Atlantic Convergence Zone (SACZ) occurs, in the Zona da Mata Arch, and in the State of Minas Gerais. Great spatial variability was also observed among the months and times for maximum occurrence throughout Brazil.

Rudlosky et al. (2019), conducted a study on the spatio-temporal distribution of lightning for the first nine operational months (December 2017 to August 2018) of the GLM sensor on board the GOES-16 satellite across the sensor's observation hemisphere. During this period, the GLM recorded 237,100,495 lightning flashes, 83% (17%) of which occurred over continental areas (oceans), and the highest occurrences were recorded for the summers in each hemisphere. Maximum rates were found between the border of Brazil and Argentina (10.6 fl km^{-2} month^{-1}), in Northern Brazil, and along the Andes Mountain range. A study by Rudlosky and Virts (2021), examined observations from the GOES-16 and 17 GLM sensor during the first 18 months of operation (December 1, 2018– May 31, 2020) and found density values above 1 fl km^{-2} month^{-1} over the continent, with high levels in Venezuela and Colombia (10 fl km^{-2} month^{-1} except in December–January-February). Both studies suggested that certain regions are more susceptible to longer duration lightning, for example, in regions where Mesoscale Convective Systems (MCSs) are found. More recently, the Meteorological Organization verified mega-flash lightning extremes (Lyons et al., 2020) in this same region, recorded by the GLM (Peterson et al., 2020). The record for flash distance occurred in southern Brazil, which was 709 km, and the record for flash duration occurred in northern Argentina, with a single flash lasting for 16.73 s. Peterson (2021), documented three years (2018–2019) of GLM Mega-Flashes, and found that all were concentrated in the central United States and in southern Brazil, in Rio Grande do Sul, and Uruguay.

Both OTD and LIS sensors were on board satellites in low orbit with elliptical and circular orbits, respectively. Therefore, it took 65 and 35 days for the satellite to return to the same point at the same time. Because of this, they did not fully monitor the same area (Christian et al., 2003; Cecil et al., 2014; Albrecht et al., 2016b), limiting the actual sampling of lightning. On the other hand, GLM continuously observes all storms within its field-of-view with the same 2 ms temporal resolution as OTD and LIS. These observations are then packed and delivered to users every 20 s. Then, these continuous storm observations can then be used to investigate many important lightning characteristics (such as FRD) using data over a shorter period of time as compared to low Earth orbit instruments such as OTD and LIS. Hence, just a few years of data can provide robust statistics to study, for example, the annual, seasonal, monthly, and daily FRD behavior. Other climatological studies, such as investigations of interannual variability, could also be carried out using shorter periods of data as compared to similar studies using OTD and LIS statistics.

Detailed lightning mapping studies using the GOES-16 satellite have not yet been conducted for Brazil. Due to the size of Brazil and the fact that it is one of the countries with the most lightning flashes in the world, studies of this nature will be very important for developing national strategies. Furthermore, lightning flashes are generally associated with severe weather events (Williams et al., 1999; Schultz et al., 2011), and knowledge on the spatio-temporal distribution is essential. These results can help improve severe weather alerts, for example. Several studies have found drastic increases in lightning, or so-called lightning jumps, moments before heavy precipitation and severe weather events, where hail, damaging winds, and tornadoes develop (Goodman et al., 1988; Williams et al., 1999; Rudlosky and Fuelberg, 2013; Schultz et al., 2011). These events can cause losses to many sectors of society.

This initial study seeks to assess the spatio-temporal distribution of total lightning flashes observed by the GLM sensor over Brazil during three-years (2018–2020) period. In the following section (Section 2), we will describe the data and methodology used. In Section 3.1, we analyze the annual and seasonal distribution of the total lightning Flash Rate Density (FRD), followed by a description of the maximum month of FRD in Section 3.2, and maximum local hour FRD in Section 3.3. We also identify and rank the Brazilian cities/regions with the highest FRD concentration, which we will call "lightning hotspots" in Section 3.4, and will study the annual and diurnal cycle in Section 3.5. The conclusions are presented in Section 4.

2. Material and methods

Total lightning flashes (intracloud + cloud-to-ground) detected using the GLM sensor on board the GOES-16 satellite for 2018, 2019 and 2020

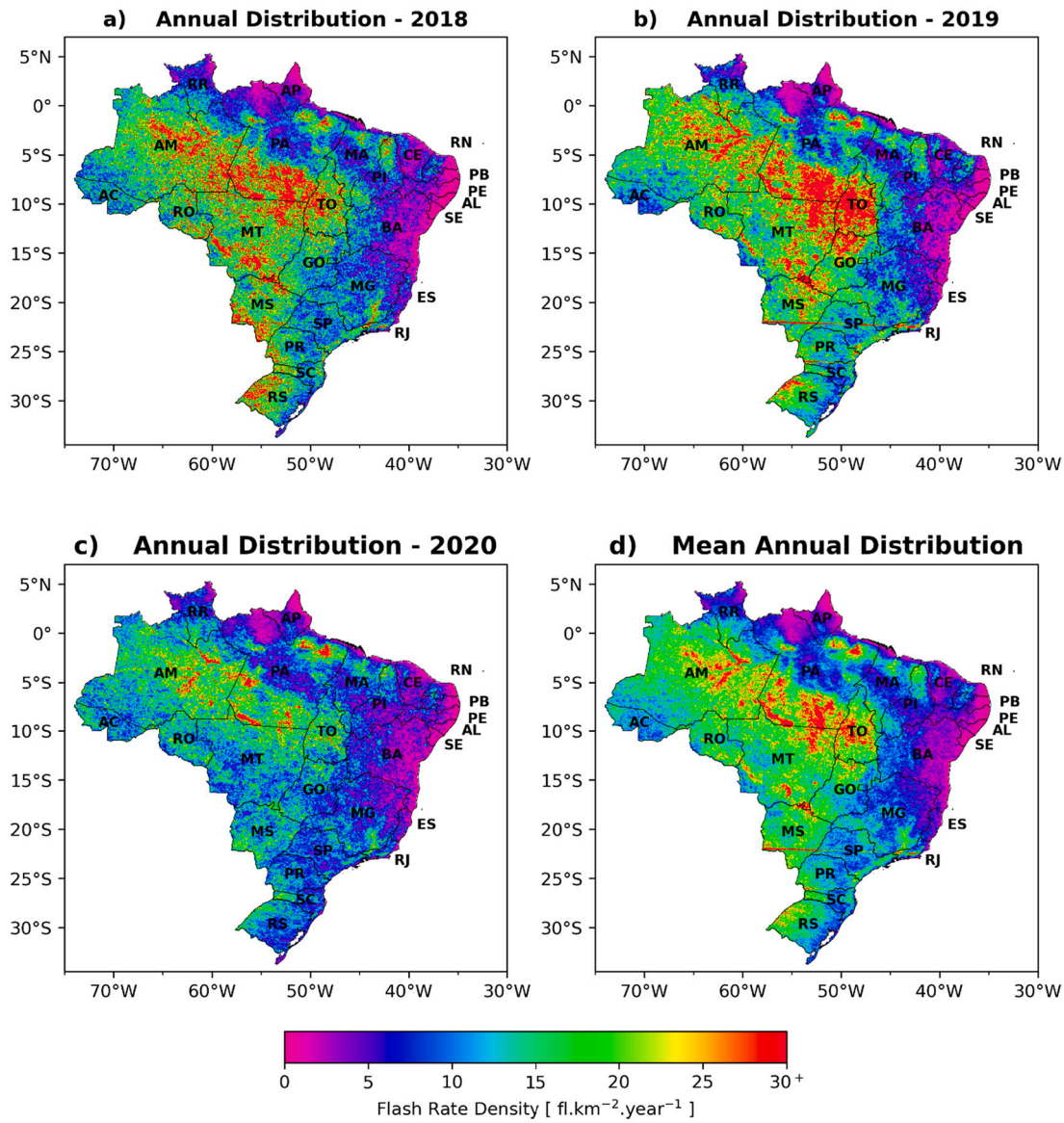

Fig. 1. Total Lightning Flash Rate Density (FRD) in (a) 2018, (b) 2019, (c) 2020 and (d) average estimated using the GLM sensor on board the GOES-16 satellite for Brazil.

were considered in this study. The GLM is the first sensor on board a geostationary satellite that can be used to map total lightning flashes with almost uniform resolution in real time, i.e., it monitors the same area continuously. This is a high-resolution sensor (1372 × 1300 pixels), and has a Charge Coupled Device (CCD) with a narrow band interference filter operating in the near infrared range (777.4 nm). Its field of view (FOV) covers most of the western hemisphere (Goodman et al., 2013). GLM pixel spatial resolution is 8 km in the nadir, reaching 14 km at the edges, and it records lightning every ~2 ms (503 frames per second), delivering a compiled data file every 20 s (Edgington et al., 2019; Peterson, 2020).

The GLM estimates the upward optical radiation emitted by lightning that crosses the tops of clouds by tracking instantaneous signal increases as compared to the average background brightness value of each pixel (Goodman et al., 2012). The expected detection efficiency exceeds 70%, and the false alarm rate is 5%. It performs better at night (90%) than during the day (70%) (Goodman et al., 2013). An extensive set of clustering and filtering algorithms are applied to the raw GLM data to remove false events and artifacts. According to Bateman and Mach (2020), the GLM detection efficiency is greater than 70%, averaged over the whole field-of-view during 24 h. However, even when using filters, false events, like solar reflections, solar intrusions during eclipses, and the brightness of relatively calm rivers, lakes, and oceans, in combination with specific angles, can be labeled as events in the algorithm (Peterson, 2020). This effect is clearly seen in the Amazon basin, as noted by Rudlosky et al. (2019).

The lightning data used in this study is from the GLM Level 2 (L2) from the GLM lightning cluster filter algorithm (LCFA) (Goodman et al., 2012). The GLM L2 files contain information on GLM events, groups, and flashes derived from the CCD array radiance measurements, and their geographical position relies on the satellite's position, which are then converted to latitude and longitude coordinates (Rudlosky et al., 2019; GOES-R Algorithm Working Group, 2017). In this study we use GLM flashes from 01 January 2018 to 31 December 2020 for all of Brazil. Only flashes with Data Quality Flags classified as "good" (i.e., flag value = 0) were used (Rudlosky et al., 2019; GOES-R Algorithm Working Group, 2017). The original data on GLM flashes is provided in 20 s packets (or bins). For this investigation, these were accumulated over 5-min bins. This processing step was carried out by the Center for Weather Forecasting and Climate Studies (CPTEC) from the National Institute for

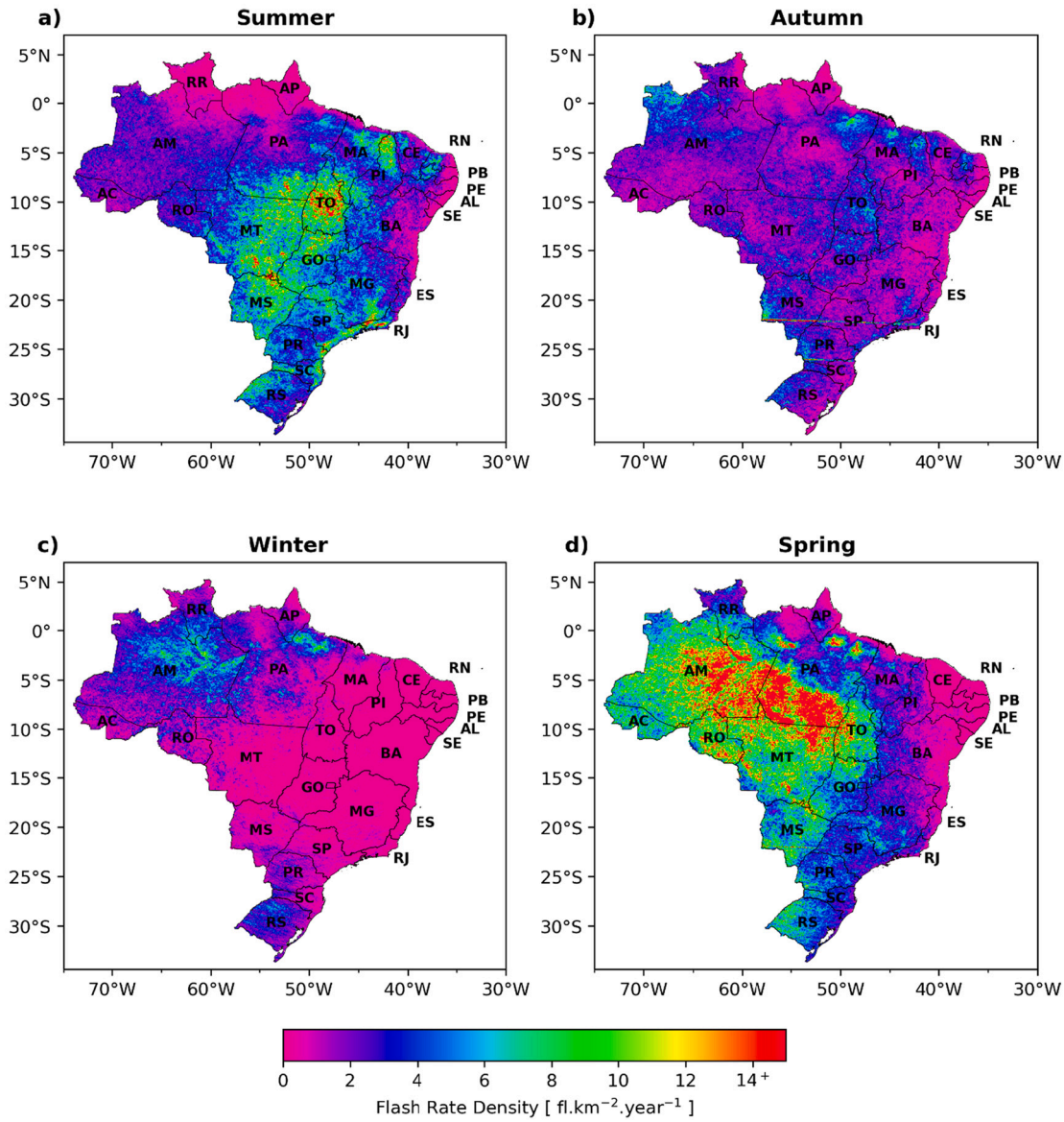

Fig. 2. Total Lightning Frequency Rate Density (FRD) per season (fl km^{-2} season^{-1}) (2018–2020) for Brazil estimated using the GLM sensor on board the GOES-16 satellite for: a) summer, b) autumn, c) winter and d) spring.

Table 1
Total of synoptic events recorded during three-year period (from 2018 to 2020) in Brazil.

Months	South Atlantic Convergence Zone (SACZ)	Humidity Coverage Zone (HCZ)	Cold Fronts	Upper Tropospheric Cyclonic Vortex (UTCV)
Jan	6	2	15	21
Feb	6	6	11	12
Mar	3	3	17	7
Apr	1	3	18	13
May	0	0	14	12
June	0	0	16	9
July	0	0	15	18
Aug	0	0	16	7
Sept	0	0	18	9
Oct	1	3	21	14
Nov	2	3	16	18
Dec	4	5	14	16
Total Annual	23	25	191	156

Source: Center for Weather Forecasting and Climate Studies (CPTEC) of the National Institute for Space Research (INPE).

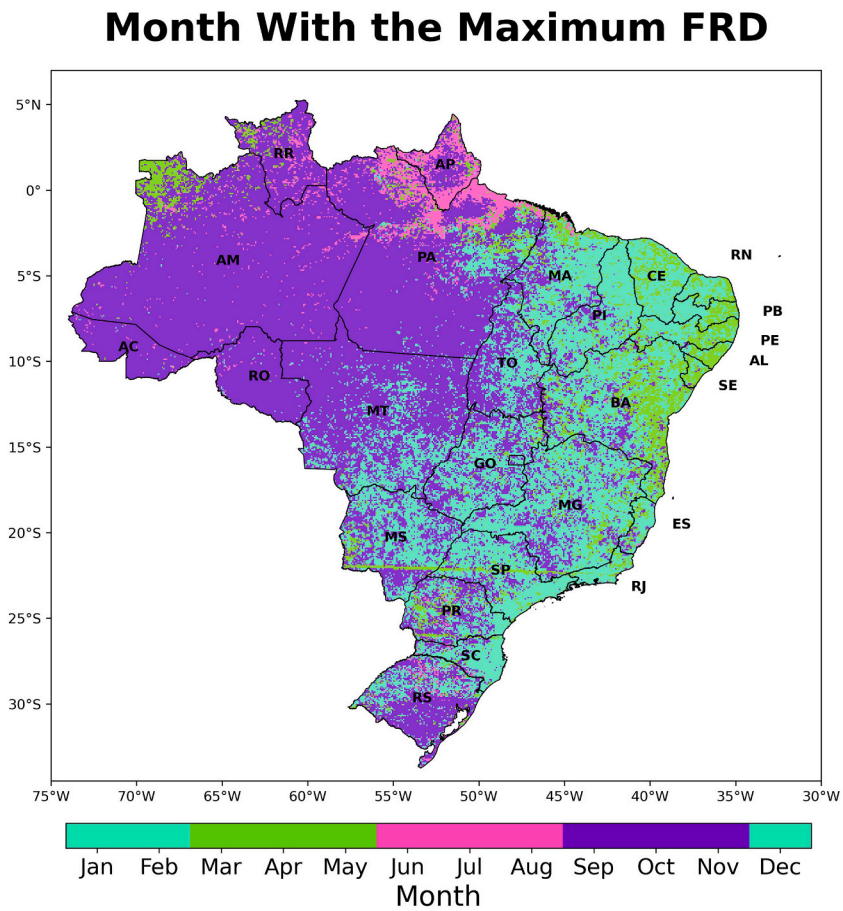

Fig. 3. Month of Maximum Total Lightning Frequency Rate Density (FRD) (2018–2020) estimated using the GLM sensor on board the GOES-16 satellite.

Space Research (INPE) and the data are available at: http://ftp.cptec.inpe.br/goes/goes16/goes16_web/glm_acumulado_nc/.

The total average lightning data (2018 to 2020) was accumulated for different time intervals (annual, seasonal, monthly, and daily) for each grid point of 8×8 km^2 of spatial resolution, corresponding to the pixel area value in the nadir. The annual analysis map for FRD is shown and discussed in Section 3.1, along with the seasonal analysis. For seasonal analysis, data were accumulated at quarterly intervals and divided into an austral summer (December–January-February), an austral autumn (March–April-May), an austral winter (June–July-August), and an austral spring (September–October-November). The seasonal distribution can show variability among each season, and in Section 3.2 we show the month with the highest frequency of total lightning per pixel, using monthly maps of accumulated FRD data. Section 3.3 shows the local hour of maximum lightning, considering the hour of maximum FRD for each pixel point. This value is taken by accumulating all lightning from the three-year period analyzed (2018 to 2020) for each 1-local hour interval, representing the total lightning per hour. Based on these data, the hour with the most total lightning for each pixel was extracted. In Section 3.4, five "lightning hotspots" were determined for the South, Southeast, Midwest, North, and Northeast regions of Brazil using the annual accumulated lightning map (average from 2018 to 2020) (Section 3.1), i.e., the five grid points (or pixels) with the highest FRD value. These pixels were associated with the closest cities. Section 3.5 presents an analysis of the diurnal and monthly cycles for the average pixel for each region and for each hotspot.

3. Results and discussion

3.1. Annual and seasonal distribution of total lightning flashes

The GLM detected an annual average of 96,446,274 lightning flashes in Brazil during the study period (2018 to 2020). 103,272,364 total lightning flashes were registered during 2018, 108,413,867 for 2019 and 77,652,591 during 2020. This corresponds to approximately 29%, 29.52% and 31.74% of the total lightning flashes detected in the entire field of view of the GOES-16 satellite for the same period, respectively.

Fig. 1 shows the spatial distribution of the total lightning flashes detected over Brazil in the FRD map from 2018 to 2020 and the average of the three years. The highest FRD values in 2018 were observed near the border between Brazil and Argentina (passing through Mato Grosso do Sul, MS; Paraná, PR; Santa Catarina, SC; and Rio Grande do Sul, RS) (30–90 fl km^{-2} year^{-1}), and in the northwest-central portion of the country (Amazonas, AM; Pará, PA; Mato Grosso, MT; and Tocantins, TO) (30–70 fl km^{-2} year^{-1}), and at the Zona da Mata Arch, Minas Gerais (MG) (about 40 fl km^{-2} year^{-1}), and at south of Rio de Janeiro (RJ) (about 38 fl km^{-2} year^{-1}), and in the northern region of PA (67–78 fl km^{-2} year^{-1}), and in Maranhão (MA) (39–49 fl km^{-2} year^{-1}), and in Piauí (PI) (37–39 fl km^{-2} year^{-1}). The year 2019 (Fig. 1b) presented a spatial behavior very similar to 2018, with small differences: it is possible to see that the amount of FRD equal to or greater than 30 fl km^{-2} year^{-1} in the border between Brazil and Argentina (MS, PR, SC and RS) and in the Arco da Zona da Mata region in MG it decreased, while in the states of PA, TO, GO and MT it increased, which contributed to the greater amount of lightning flashes total detected in 2019 compared to 2018 (an increase of 4.98%). In general, the year 2020 presented low FRD than previous two years (decrease of 24.81%

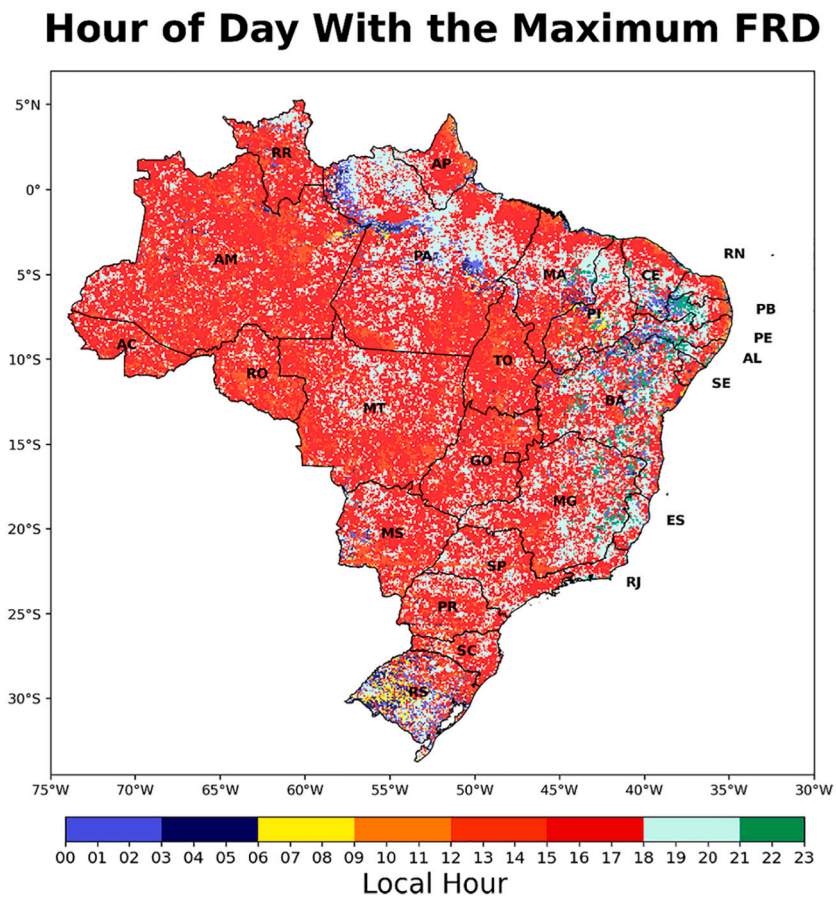

Fig. 4. Local Hour of Maximum Total Lightning Frequency Rate Density (FRD) (2018–2020) estimated using the GLM sensor on board the GOES-16 satellite.

compared to 2018), keeping only values greater than or equal to 30 fl km^{-2} year^{-1} in some locations in PA, AM, MT, TO and MG.

The three-year average evidenced the difference in the spatial behavior of the FRD distribution in the East (lower FRD values) and West (higher FRD values) portions of the country (Fig. 1d). Overall, these observations corroborate the results found in climatology studies by Christian et al. (2003), using OTD sensor data, and by Cecil et al. (2014), when merging OTD and LIS data. Albrecht et al. (2016a), used LIS sensor data and Rudlosky et al. (2019), studied the first nine months of GLM operation.

Of the total annual lightning flashes, 29.55% occurred in austral summer (DJF), 15.65% occurred in austral autumn (MAM), 9.55% occurred in austral winter (JJA) and 45.24% occurred in austral spring (SON). Fig. 2 shows the seasonal spatial distribution from the three-year average (2018–2020). In the austral summer (Fig. 2a), the highest FRD (>14 fl km^{-2} year^{-1}) occurred in the northeast (MA and PI), in the central portion of Brazil (south of PA, TO, MT, GO, MS), in the south portion (southeast of MG, RJ, and near the coast - SP, PR and SC). At this time of year, convective activity is influenced by the migration of the main radiative warming zone to the subtropics. Also suffers influence by the intensification of the northeastern trade winds, carrying more moisture from the Atlantic Ocean to the Amazon Basin region. This humidity, in turn, is transported to the southern region of Brazil via the South American Low-Level Jet (LLJ) (Virji, 1981; Berri and Inzunza, 1993; Sugahara et al., 1994), and plays an important role in positioning the South Atlantic Convergence Zone (SACZ) in southeastern Brazil (Nogués-Paegle and Mo, 1997; Seluchi and Marengo, 2000; Cazes-Boezio et al., 2003).

In the autumn (Fig. 2b), the spatial distribution is more homogeneous with high FRD (6 to 14 fl km^{-2} year^{-1}) in the states of MS, PR, RJ, MG. Of the 4 seasons of the year, it is in autumn (Fig. 2b) that two lines of high FRD can be clearly identified. The first line crosses the states of MS, SP, MG and SP; and the second line is located in PR and SC states. As observed by Rudlosky et al. (2019), this information influenced the annual accumulated of 2018, 2019 and the average of the three years. By contrast, due to the decrease in surface warming, and the intensification of the South Atlantic Subtropical Anticyclone (SASA) (Reboita et al., 2019) in winter (Fig. 2c), lightning activity in Brazil reached a minimum value, and the spatial distribution became more heterogeneous, with little to no lightning from the northeast coast towards central Brazil. However, three regions with FRD between 4 and 8 fl km^{-2} year^{-1} should be mentioned, the central Amazon region and PA, resulting from the strengthening of trade winds (Uvo and Berndtsson, 1996), which enter the continent carrying moisture, and also southern Brazil, due to cold front incursion (Satyamurty and Mattos, 1989; Rodrigues et al., 2004).

During the spring (Fig. 2d), maximum (30 fl km^{-2} year^{-1}) FRD values are observed mainly in western portion of the north (in the central and southeastern region of the Amazon Basin, PA, TO, RO), while little to no lightning was observed in the northeastern region of Brazil. This corroborates results from Gin and Guedes (2000), in a climatology study carried out using 10 years' worth of data on observed lightning and/or thunder at surface meteorological stations. In summary, there was a shift of the maximum FRD from the northwest portion of Brazil (austral spring) to the central region of Brazil (austral summer), and this shift is possibly caused by the seasonal variation of convection driven by solar radiation that is more concentrated in the north of the country during winter and spring and moves south during summer (Funari and Tarifa, 2017), which is associated with the interanual variablility of the South American Monsoon System (Raia and Cavalcanti, 2008).

In South America there is high seasonal variable precipitation, characteristic of a monsoon system with rainy summers and dry winters (Zhou and Lau, 1998). Likewise, this pattern is seen in Fig. 2, with high

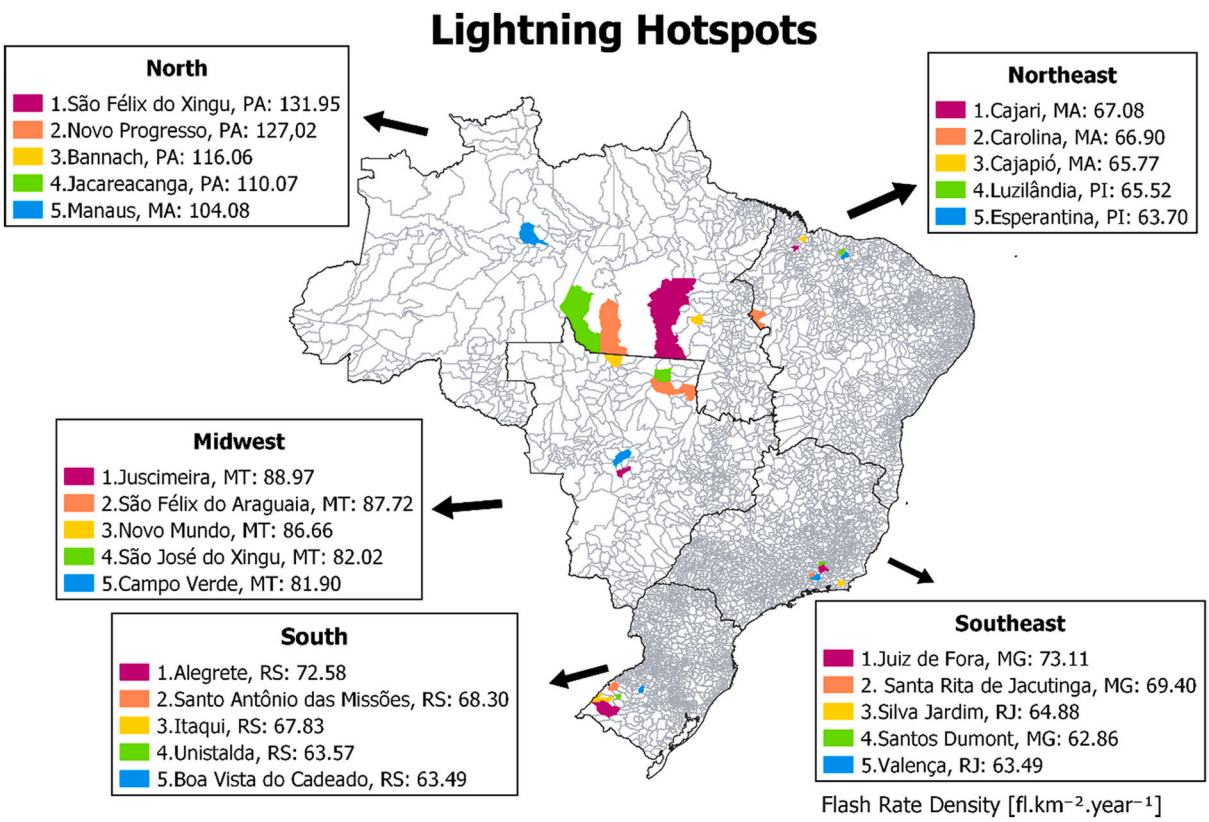

Fig. 5. The first five hotspots (cities with maximum Total Lightning FRD) for each Brazilian geopolitical region (2018–2020), estimated using the GLM sensor on board the GOES-16 satellite. The numbers inside the boxes represents the FRD values (fl km^{-2} year^{-1}). Gray and black lines are the city and geopolitical boundaries, respectively.

seasonal variability and lightning occurrences. Since precipitation is most often accompanied by lightning (Battan, 1965; Kinzer, 1974; Buechler and Goodman, 1990; Williams et al., 1992; Tapia et al., 1998; Soula and Chauzy, 2001), it is plausible to associate lightning and convective processes. Therefore, the patterns of occurrence can vary according to the region and the meteorological systems that act on the region.

For example, in the north, precipitation is characterized by the seasonal displacement of the Intertropical Convergence Zone (ITCZ) (Nobre, 1983; Marengo and Hastenrath, 1993), by the formation of Squall Lines (SL) along the coast and within the Amazon Basin (Kousky, 1980), by frontal systems that penetrate into southern Amazônia (Kousky and Ferreira, 1981; Fisch et al., 1998), by the formation of tropical MCSs (Salio et al., 2007), and by the displacement of the South Atlantic Subtropical High (SASH) and the Bolivian High (BH) (Virji, 1981). In northern Brazil, the ITCZ (Utida et al., 2019), Cold Fronts (CF) in the south of Bahia (from November to February), Easterly Waves (Yamazaki and Rao, 1977; Torres and Ferreira, 2011; Gomes et al., 2019), SACZ activity (southern region of northeast Brazil) (Chaves and Cavalcanti, 2001), the Upper Tropospheric Cyclonic Vortex (UTCV) (Coutinho et al., 2010; Fedorova et al., 2018), and sea breezes (May to June) (Kousky, 1979), are responsible for maximum rainfall in the region.

The South region presents a uniform annual rainfall distribution due to the constant incursion of frontal systems (Kousky, 1979; Gan and Rao, 1991; Rodrigues et al., 2004; Amorim Neto et al., 2015), and the presence of an inverted trough over the northwest-southeast of Rio Grande do Sul to Santa Catarina, mainly in spring and summer (Fernandes and Satyamurty, 1994), cyclonic systems (Bonatti and Rao, 1987; Iwabe and Da Rocha, 2009), atmospheric blocking (Nascimento and Ambrizzi, 2002; Silva et al., 2015), MCSs (Custódio and Herdies, 1994; Salio et al., 2007), UTCV (Matsumoto et al., 1982), sea breezes (Braga and Krusche, 2000) and the SACZ (Quadro and Abreu, 1994; Nogués-Paegle and Mo, 1997).

Additionally, we visually analyzed surface and altitude synoptic charts (250 hPa) provided by the Center for Weather Forecasting and Climate Studies (CPTEC) from the National Institute for Space Research (INPE). The objective was to account for SACZ, HCZ (Humidity Coverage Zone, (Sacramento Neto et al., 2010), CF, and UTCV in 2018, 2019 and 2020 in Brazil (Table 1). Throughout the period analyzed, both SACZ and HCZ were predominantly positioned further north, in AM, MT, GO, MG, TO and PA, as was already observed by other studies (Kodama, 1992; Liebmann et al., 1999; Sacramento Neto et al., 2010). About 20% of cold front incursions in the country reached the northeast during the autumn and winter months. Most UTCV occurred in the northeast, more specifically in BA, RN, CE, PB and PE.

3.2. Month of maximum total lightning

Following Albrecht et al. (2016a), monthly FRD maps were computed, and Fig. 3 shows the spatial distribution of the month with the highest FRD. One can see that in the western portion of Brazil, the highest FRD occurs predominantly in the months of winter to spring and at the eastern portion, and in the summer to autumn. More homogeneous distributions were concentrated in the north and south of Brazil. These patterns confirm the presence of atmospheric systems on a seasonal scale, as discussed in the previous section. For example, Gin and Guedes (2000), found that regions with the greatest occurrences of lightning from January to March, were Manaus, Brasília, São Luís, and Belém. Albrecht et al. (2016a), gave maximum FRD values for the summer and autumn months in the eastern region of Brazil, and maximum FRD values for the winter and spring months in the western

Table 2
Geographic location, placement in the regional and national rankings, and FRD (fl km^{-2} year^{-1}) values for each regional hotspot in Brazil considering three-year period (from 2018 to 2020) estimated using the GLM sensor on board the GOES-16 satellite.

Regional Ranking	National Ranking	City	State	Lat	Lon	FRD
		North				
1°	1°	São Félix do Xingu	PA	−8.48	−52.28	131.95
2°	2°	Novo Progresso	PA	−9.20	−55.88	127.02
3°	3°	Bannach	PA	−7.60	−51.00	116.06
4°	4°	Jacareacanga	PA	−8.56	−57.16	110.07
5°	5°	Manaus	AM	−2.56	−60.68	104.08
		Northeast				
1°	144°	Cajari	MA	−3.36	−45.08	67.08
2°	148°	Carolina	MA	−7.20	−47.40	66.90
3°	157°	Cajapió	MA	−2.96	−44.60	65.77
4°	162°	Luzilândia	PI	−3.68	−42.44	65.52
5°	188°	Esperantina	PI	−3.40	−42.36	63.70
		Midwest				
1°	21°	Juscimeira	MT	−16.32	−55.08	88.97
2°	23°	São Félix do Araguaia	MT	−11.12	−53.08	87.72
3°	25°	Novo Mundo	MT	−9.60	−55.80	86.66
4°	33°	São José do Xingu	MT	−10.88	−53.08	82.02
5°	36°	Campo Verde	MT	−15.84	−55.40	81.90
		Southeast				
1°	76°	Juiz de Fora	MG	−21.68	−43.64	73.11
2°	117°	Santa Rita de Jacutinga	MG	−22.16	−44.04	69.40
3°	173°	Silva Jardim	RJ	−22.56	−42.60	64.88
4°	202°	Santos Drumont	MG	−21.44	−43.64	62.86
5°	212°	Valença	RJ	−22.24	−44.04	62.36
		South				
1°	81°	Alegrete	RS	−29.84	−55.88	72.58
2°	126°	Santo Antônio das Missões	RS	−28.48	−55.56	68.30
3°	138°	Itaqui	RS	−29.20	−56.52	67.83
4°	190°	Unistalda	RS	−29.12	−55.08	63.57
5°	192°	Boa Vista do Cadeado	RS	−28.48	−53.80	63.49

region of Brazil. However, these data have smoothed out climatology data collected over 16 years.

Comparing Figs. 1 and 3, one can see that regions in the extreme north of Brazil have the lowest lightning levels, but had higher levels in the winter months. The northeast region of Brazil also showed little annual accumulation for high FRD values, predominantly in the summer and in the autumn, showing that formations depend on radiative heat to generate electrical activity in the area. However, regions with higher densities were more influenced by electrical activity in the winter and spring months. In the Amazon, the transition between the dry-to-wet season (September to November) showed strong thunderstorm formation and higher electrical activity (Williams et al., 2002; Albrecht et al., 2011). By contrast, RS and the eastern portions of MS, PR and SC were influenced by electrical activity from both the MCS and frontal systems (Anabor, 2008).

3.3. Local hour of maximum total lightning flashes

Map on local hour FRD were computed, and Fig. 4 shows the spatial distribution of the local hour with the highest FRD. In general, most total lightning strokes occurred between 12 and 18 Local Hour(LH) intrinsically related to daytime radiative heating. However, part of the northeast coast (09 to 12 LH), the central-south region (no preferred time), and an extensive line extending 500 to 1000 km inland, parallel to the coast in north-northeast region (18 to 23 and from 00 to 03 LH) had maximum FRD levels occurring at different times during the day. This can be attributed to the different meteorological systems present in each region of Brazil. For example, the northeast coast is highly influenced by sea breezes (Kousky, 1979), and according to Albrecht et al. (2016a), the southern region of the northeast Brazil coast is influenced by cold fronts that occur throughout the year, and during all times of the day, i.e., they do not have a well-defined annual and hourly cycle. Southern Brazil is also affected by frontal systems (Gan and Rao, 1991), and registered no preferential time for lightning activity. Here lightning is slightly more predominant in the early morning due to the passage of decaying MCSs and an intensified LLJ (Custódio and Herdies, 1994). The "break" in afternoon convection at 500–1000 km inland, parallel to the coast in the north-northeastern region, showed nighttime lightning maximums (in Fig. 4), and this can be associated with the Amazon Coastal Squall Lines (ACSL - Cohen et al., 1995) propagating from the east, associated with the ACSL (e.g., Garstang et al., 1994; Albrecht et al., 2016a). However, more recently, Anselmo et al. (2020, 2021), showed that it is less common for the ACSL to cross this region, and this break may be related to the diurnal cycle of the Amazon Low Level Jet, by advecting humidity from the coast overnight to assist in daytime convection the following day, or due to internal gravity waves.

In the southeast, lightning strokes occur predominantly in late afternoon to early evening. This can be explained by the action of sea breezes that destabilize air, formatting intense convective systems (Salio et al., 2007).

3.4. FRD hotspots for five geopolitical regions in Brazil

In this section we analyze lightning hotspots for the average FRD from 2018 to 2020. We divided Brazil into its main five geopolitical regions, the South, the Southeast, the Midwest, the Northeast, and the North, as shown in Fig. 5, and in Table 2. It is noteworthy that the hotspots in the Midwest, Southeast and South were influenced by the lines observed in Figs. 1 and 2 in the states of MS, SP, MG, SP and in PR and SC. Fig. 5 also highlights the first five regions with lightning hotspots per each region. The largest FRD level was registered for São Félix do Xingu (PA), at approximately 131 fl km^{-2} year^{-1}. These observations confirm synoptic systems that occur in each region. Albrecht et al. (2016a), found similar results, for maximum FRD in Brazil using data from the LIS sensor, but their maximum value was found near Manaus, on the eastern border of the Rio Negro River.

The northeastern region showed heterogeneous distribution, with minimal (0–27.95 fl km^{-2} year^{-1}) densities concentrated along coastal areas (Fig. 1), where convective activity is lower, and where warm clouds prevail (Palharini and Vila, 2017). In general, PI, MA and BA showed the most lightning strokes in northeast (Abreu et al., 2020), and the 5 hotspots are concentrated mainly in MA and PI, at low-altitude cities. According to Kousky and Gan (1981), vortices that penetrate Brazil, mostly closer to Salvador (BA), are responsible for convective activity in the north and for good weather in the south and central regions of the northeast. This is directly associated with lightning.

3.5. Monthly and daytime distribution of total lightning for hotspots

Fig. 6 shows the monthly cycle of FRD for the 5 regions of the country, the left column being represented by the monthly cycle of the average pixel in each region, while the right column represents the monthly cycle of the 5 hotspots in each region. In general, with the exception of the South, all regions alternate a well-defined monthly cycle throughout the year (higher values in the spring-summer months and lower values in the winter months). In average terms (comparing the left column with the right), the hotspots of the North, Northeast and Southeast regions represent well the behavior of the FRD distribution of the region as a whole, which is not observed for the Midwest and the South.

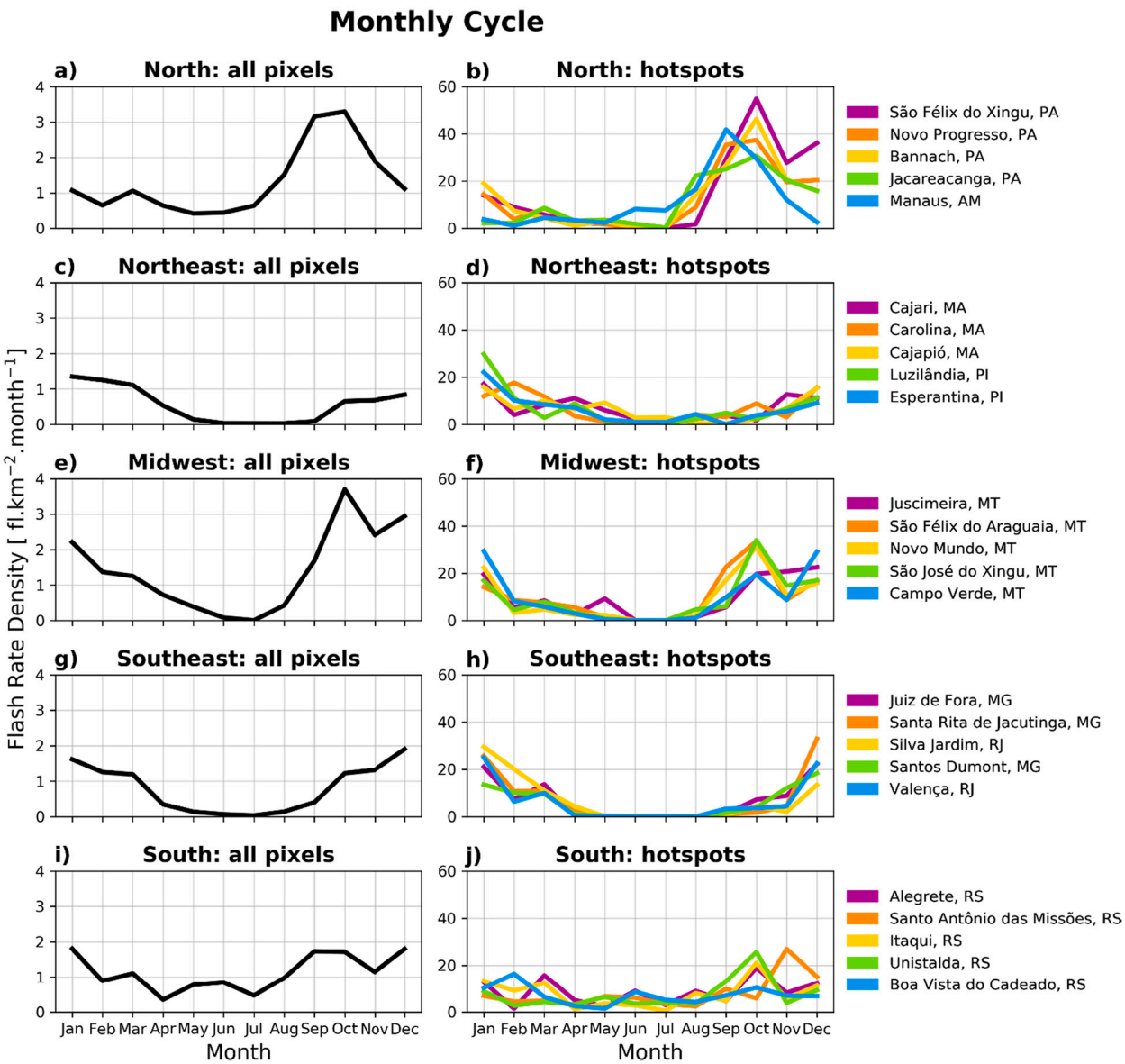

Fig. 6. Monthly Cycle of Lightning Frequency Rate Density (FRD) for the five (North, Northeast, Midwest, Southeast and South) regions of Brazil: (a, c, e, g and i) all pixels and (b, d, f, h and j) hotspots cities.

The FRD distribution in the North region (Fig. 6a and b) had higher FRD values from August, reaching its maximum in the month of October (about fl km^{-2} month^{-1}). The electrical activity in the Northeast region (Fig. 6c and d) starts in September and ends in May, with a peak of FRD in January (about 30 fl km^{-2} month^{-1}). The FRD cycle in the Midwest region (Fig. 6e and f) started from July, reaching its maximum in October (about 30 fl km^{-2} month^{-1}) and starting to decrease from February, reaching the minimum between June and July. The Southeast had one of the best-defined monthly cycles (spring and summer with higher FRD values and autumn and winter with lower values - Fig. 6g), the 5 hotspots (Fig. 6h) identified had their maximum values between December and January. The South region did not have a well-defined cycle like other regions, the hotspots (Fig. 6j) did not have a preferential month of maximum electrical activity, a behavior that represents the average cycle in the region (Fig. 6i).

We can see that cities in the first position in the ranking had more than one occurrence of pronounced peak electrical activity (Fig. 6). In general, most lightning activity has been documented for warm seasons (e.g., between spring and summer), when there is greater convective activity.

Similar to the monthly cycle analysis, Fig. 7 compares the average diurnal cycle behavior of each region of the country with the diurnal cycle behavior of each hotspot city. In a quick visual analysis it is possible to see a pattern for the 5 regions (Fig. 7a, c, e, g, i), the daytime electrical activity tends to start from 12 LH and present its maximum after 16 LH, this behavior was also observed in most hotspots, especially in the North, Northeast and Southeast regions (Fig. 7b, d, h), showing that FRD depends on solar diurnal heating. These results confirm the times of the day when meteorological systems are present in each region.

The maximum FRD values of the hotspots in the Midwest region did not have common preferential hours, despite being concentrated in the afternoon and early evening. The hotspots in the South region did not have a well-defined diurnal cycle: Alegrete peaked at 21 LH, Santo Antônio das Missões at 03 LH, Itaqui at 22 LH, Unistalda at 23 LH and Boa Vista do Cadeado at 15 LH. Both regions are affected by the occurrence of MCS.

Similarly, in the south, Azambuja (2017), found that electrical activity tended to accompany daytime sunlight, while in the in the winter and spring, activity increased at night. In the winter, there were more

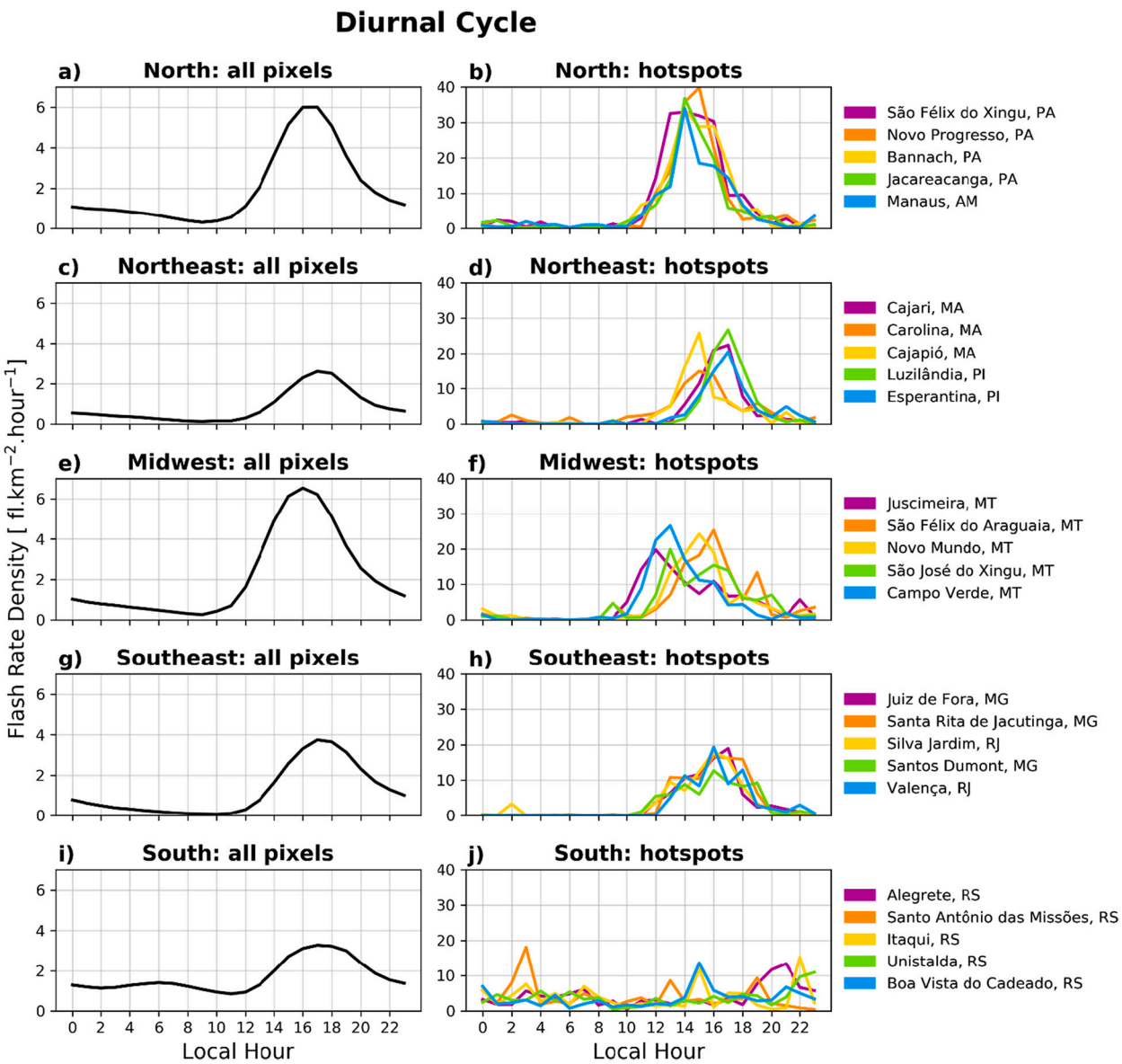

Fig. 7. Diurnal Cycle of Lightning Frequency Rate Density (FRD) for the five (North, Northeast, Midwest, Southeast and South) regions of Brazil: (a, c, e, g and i) all pixels and (b, d, f, h and j) hotspots cities.

frontal systems in the region, and in the spring the MCC formed a large horizontal front that lasted for several hours. Similarly, Ávila et al. (2015), studied 12 years' worth of data (1998–2010) from the LIS/TRMM between 25° S and 35° S and 50° W and 70° W, and reported that lightning was more frequent during due to the MCC.

4. Conclusions

This initial study analyzed the spatio-temporal distribution of Total Lightning FRD for all of Brazil using a three-year (2018 to 2020) period of data, to find the cities were lightning occurs the most among five distinct regions in Brazil. This study is pioneering in that it analyzed full three-year of lightning data estimated using a geostationary satellite, and associated this data with meteorological weather systems in Brazil. This sensor has enabled, for the first time, researchers to observe lightning activity with almost uniform resolution in real time and with a field of view that covers most of the Western Hemisphere.

This analysis allowed us to characterize the annual, seasonal, monthly, and daily lightning levels in Brazil, and to determinate five lightning hotspots in Brazil for 2018, 2019 and 2020, contributing to a better understanding of the electrical activities of these regions. This knowledge is essential for assisting severe weather alert systems, and creating public policies to minimize problems associated with lightning flashes.

The evaluation on the annual distribution of maximum lightning showed densities in the northwest-southeastern portion of the country (AM, PA, MT, GO and TO), in the southeastern of RJ and closer to the Brazil-Argentina border (MS, PR, SC and RS). The lowest FRD values were observed along coastal regions, extending from the north of RJ to AP, and for the north of RO and PA.

The evaluation of seasonal distribution showed that of the 96,446,274 lightnings flashes (three-year average) 29.55% of all lightning flashes occurred during the austral summer (DJF), 15.65% during the autumn (MAM), 9.55% during the winter (JJA) and 45.24% during the spring (SON). Maximum values occurred in DJF, in the northeast (MA and PI), in the central portions of the country (south of PA, TO, MT, GO, MS) and in the south portion (southeast of MG, RJ, and near the coast - SP, PR and SC). In the austral autumn, given temperature

decrease, the atmosphere becomes more stable, making the spatial distribution more homogeneous. By contrast, in the winter, the frequency of total lightning flashes reaches a minimum level and the spatial distribution becomes more heterogeneous, focusing on the Amazon region. Finally, in the spring, maximum values are observed mainly in the western portion of the north (in the central and southeastern region of the Amazon Basin, PA, TO, RO). In summary, there was a shift of maximum frequency from the more northwestern parts of Brazil (spring) to the central region of the country (summer).

During the evaluation of the month with maximum activity, we observed that most FRD occurred in the spring-summer (western sector of the country), and in summer-autumn (eastern sector). In the assessment on daytime distribution, generally, the majority of total lightning flashes occur in the afternoon, between 12 and 18 LH, associated with the daylight heating cycle. However, lightning flashes are prevalent in the early hours of the day in the southern regions of Brazil, probably due to MCS nighttime trends.

São Félix do Xingu city in Pará, had the highest FRD level at approximately 131 fl km^{-2} $year^{-1}$. The monthly cycles demonstrated that North, Northeast, Midwest and Southeast regions presented a well-defined monthly cycle throughout the year (higher values in the spring-summer months and lower in the winter months), while, in average terms, the hotspots in the North regions, Northeast and Southeast represent well the behavior of the FRD distribution in the region as a whole. Such behavior is not observed in the Midwest and South regions (both affected by the formation of MCS). The differential behavior between the hotspot cities, in terms of the diurnal cycle, is noteworthy. For example, maximum values were between 12 LH, with peaks from 16 LH in the North, Northeast and Southeast regions. The Midwest and South regions did not have preferred times for the peaks of FRD among their hotspots.

Future studies could analyze the impacts of different meteorological weather systems for each region in Brazil, and relate this data to lightning events.

Funding

This work was supported by the National Council for Scientific and Technological Development (CNPq) [grant numbers 438638/2018-2, 427673/2018-6 and 311457/2017-7].

CRediT authorship contribution statement

Paula S.S. Oda: Conceptualization, Methodology, Visualization, Writing – original draft, Writing – review & editing. **Diego P. Enoré:** Visualization, Writing – review & editing. **Enrique V. Mattos:** Conceptualization, Methodology, Supervision, Writing – review & editing. **Weber A. Gonçalves:** Conceptualization, Methodology, Writing – review & editing. **Rachel I. Albrecht:** Writing – review & editing.

Declaration of Competing Interest

The authors declare that they have no known competing financial interests or personal relationships that could have appeared to influence the work reported in this paper.

Acknowledgements

We would like to thank the National Oceanic and Atmospheric Administration (NOAA) for providing the GOES-16 satellite lightning data, and the Center for Weather Forecasting and Climate Studies (CPTEC) from the National Institute for Space Research (INPE) for their support and computational infrastructure for processing the GOES-16 satellite data. We would like to thank Richard J. Blakeslee (NASA Marshall Space Flight Center) and one other anonymous reviewer for theirs helpful comments.

References

Abreu, L., Gonçalves, W., Mattos, E., Albrecht, R., 2020. Assessment of the total lightning flash rate density (FRD) in northeast Brazil (NEB) based on TRMM orbital data from 1998 to 2013. Int. J. Appl. Earth Obs. Geoinf. 93, 102195 https://doi.org/10.1016/j.jag.2020.102195.

Albrecht, R., Morales, C., Silva Dias, M., 2011. Electrification of precipitating systems over the Amazon: Physical processes of thunderstorm development. J. Geophys. Res. Atmos. 116 https://doi.org/10.1029/2010JD014756.

Albrecht, R., Cecil, D., Goodman, S., 2014. Lightning. Encyclopedia of remote sensing. In: Njoku, E.G. (Ed.), Encyclopedia of Earth Sciences Series. Springer, pp. 339–344.

Albrecht, R., Goodman, S., Buechler, D., Blakeslee, R., Christian, H., 2016a. Where are the lightning hotspots on earth? Bull. Am. Meteor. Soc. 97, 2051–2068. https://doi.org/10.1175/BAMS-D-14-00193.1.

Albrecht, R., Goodman, S., Buechler, D., Blakeslee, R., Christian, H., 2016b. Supplement of where are the lightning hotspots on earth? Bull. Am. Meteorol. Soc. 97 https://doi.org/10.1175/BAMS-D-14-00193.2.

Amorim Neto, A., Satyamurty, P., Correia, F., 2015. Some observed characteristics of frontal systems in the Amazon Basin. Meteorol. Appl. 22, 617–635. https://doi.org/10.1002/met.1497.

Anabor, V., 2008. Sistemas Convectivos de Mesoescala no sul da América do sul: Propagação em Série Contra o Escoamento em Baixos Níveis. Universidade Federal de Santa Maria.

Anselmo, E., Schumacher, C., Machado, L., 2020. The amazonian low-level jet and its connection to convective cloud propagation and evolution. Mon. Weather Rev. 148, 4083–4099. https://doi.org/10.1175/MWR-D-19-0414.1.

Anselmo, E., Machado, L., Schumacher, C., Kiladis, G., 2021. Amazonian mesoscale convective systems: Life cycle and propagation characteristics. Int. J. Climatol. 1–14. https://doi.org/10.1002/joc.7053.

Ávila, E., Bürgesser, R., Castellano, N., Nicora, M., 2015. Diurnal patterns in lightning activity over South America. J. Geophys. Res. 120, 3103–3113. https://doi.org/10.1002/2014JD022965.

Azambuja, R., 2017. Estudo da Atividade de Relâmpagos na Região sul do Brasil a Partir de Dados de Sistema de Detecção. Instituto Nacional de Pesquisas Espaciais.

Bateman, M., Mach, D., 2020. Preliminary detection efficiency and false alarm rate assessment of the Geostationary Lightning Mapper on the GOES-16 satellite. J. Appl. Remote. Sens. 14, 1. https://doi.org/10.1117/1.jrs.14.032406.

Battan, L., 1965. Some factors governing precipitation and lightning from convective clouds. J. Atmos. Sci. 22, 79–84. https://doi.org/10.1175/1520-0469(1965)022<0079:SFGPAL>2.0.CO;2.

Berri, G., Inzunza, J., 1993. The effect of the low-level jet on the poleward water vapour transport in the central region of South America. Atmos. Environ. Part A. General Topics. 27, 335–341. https://doi.org/10.1016/0960-1686(93)90107-A.

Boccippio, D., Goodman, S., Heckman, S., 2000. Regional differences in tropical lightning distributions. J. Appl. Meteorol. 39, 2231–2248. https://doi.org/10.1175/1520-0450(2001)040<2231:RDITLD>2.0.CO;2.

Bonatti, J., Rao, V., 1987. Moist baroclinic instability in the development of North Pacific and South American intermediate-scale disturbances. J. Atmos. Sci. 44, 2657–2667. https://doi.org/10.1175/1520-0469(1987)044<2657:MBIITD>2.0.CO;2.

Bourscheidt, V., Cummins, K., Pinto Jr., O., Naccarato, K., 2012. Methods to overcome lightning location system performance limitations on spatial and temporal analysis: Brazilian case. J. Atmos. Ocean. Technol. 29, 1304–1311. https://doi.org/10.1175/JTECH-D-11-00213.1.

Braga, M., Krusche, N., 2000. Estudo comparative entre dois métodos de medição de direção e velocidade do vento na região de Rio Grande-RS. In: Congresso Brasileiro De Meteorologia, 11, pp. 2400–2408.

Brooks, C., 1925. The distribution of thunderstorms over the globe. Geophys. Memoirs. 3, 147–164.

Buechler, D., Goodman, S., 1990. Echo size and asymmetry: Impact on NEXRAD storm identification. J. Appl. Meteorol. 29, 962–969. https://doi.org/10.1175/1520-0450(1990)029<0962:ESAAIO>2.0.CO;2.

Cardoso, I., Pinto Jr., O., Pinto, I., Holle, R., 2014. Lightning casualty demographics in Brazil and their implications for safety rules. Atmos. Res. 135–136, 374–379. https://doi.org/10.1016/j.atmosres.2012.12.006.

Cazes-Boezio, G., Robertson, A., Mechoso, C., 2003. Seasonal dependence of ENSO teleconnections over South America and relationships with precipitation in Uruguay. J. Clim. 16, 1159–1176. https://doi.org/10.1175/1520-0442(2003)16<1159:SDOETO>2.0.CO;2.

Cecil, D., Buechler, D., Blakeslee, R., 2014. Gridded lightning climatology from TRMM-LIS and OTD: Dataset description. Atmos. Res. 135–136, 404–414. https://doi.org/10.1016/j.atmosres.2012.06.028.

Chaves, R., Cavalcanti, I., 2001. Atmospheric circulation features associated with rainfall variability over Southern Northeast Brazil. Mon. Weather Rev. 129, 2614–2626. https://doi.org/10.1175/1520-0493(2001)129<2614:ACFAWR>2.0.CO;2.

Christian, H., Blakeslee, R., Boccippio, D., Boeck, W., Buechler, D., Driscoll, K., Goodman, S., Hall, J., Koshak, W., Mach, D., Stewart, M., 2003. Global frequency and distribution of lightning as observed from space by the Optical Transient Detector. J. Geophys. Res. 108, 4005. https://doi.org/10.1029/2002JD002347.

Cohen, J., Silva Dias, M., Nobre, C., 1995. Environmental conditions associated with amazonian squall lines: a case study. Mon. Weather Rev. 123, 3163–3174. https://doi.org/10.1175/1520-0493(1995)123<3163:ECAWAS>2.0.CO;2.

Coutinho, M., Gan, M., Rao, V., 2010. Método objetivo de identificação dos vórtices ciclônicos de altos níveis na região tropical sul: Validação. Rev. Bras. Meteor. 25, 311–323.

Cummins, K., Murphy, M., Bardo, E., Hiscox, W., Pyle, R., Pifer, A., 1998. A combined TOA/MDF technology upgrade of the US National Lightning Detection Network. J. Geophys. Res. 103, 9035–9044. https://doi.org/10.1029/98JD00153.

Custódio, M., Herdies, D., 1994. O jato de baixos níveis a leste da Cordilheira dos Andes – um estudo de caso. In: VIII Congresso Brasileiro de Meteorologia (SBMET), 2, pp. 617–619.

Edgington, S., Tillier, C., Anderson, M., 2019. Design, calibration, and on-orbit testing of the geostationary lightning mapper on the GOES-R series weather satellite. In: International Conference on Space Optics (ICSO), 11180, p. 1118040. https://doi.org/10.1117/12.2536063.

Fedorova, N., Levit, V., Campos, A., 2018. Brazilian Northeast Jet Stream: association with synoptic-scale systems. Meteorol. Appl. 25, 261–268. https://doi.org/10.1002/met.1693.

Fernandes, K., Satyamurty, P., 1994. Cavados invertidos na região central da América do Sul. In: II Congresso Brasileiro de Meteorologia, Belo Horizonte, 8, pp. 93–94.

Fisch, G., Marengo, J., Nobre, C., 1998. Uma revisão geral sobre o clima da Amazônia. Acta Amazon. 28 (101–101).

Funari, F., Tarifa, J., 2017. Insolação, radiação solar global e radiação líquida no Brasil. Revista do Instituto Geológico 38 (2), 49–83. https://doi.org/10.5935/0100-929X.2017000947698001.

Fuquay, D., 1982. Positive cloud-to-ground lightning in summer thunderstorms. J. Geophys. Res. 87, 7131–7140. https://doi.org/10.1029/JC087iC09p07131.

Gan, M., Rao, V., 1991. Surface cyclogenesis over South America. Mon. Weather Rev. 19, 1293–1302.

Garstang, M., Massie Jr., H., Halverson, J., Greco, S., Scala, J., 1994. Amazon coastal squall lines. Part I: Structure and kinematics. Mon. Weather Rev. 122 (4), 608–622. https://doi.org/10.1175/1520-0493(1994)122<0608:ACSLPI>2.0.CO;2.

Gin, R., Guedes, R., 2000. Climatologia de Relâmpagos No Brasil: Análise Preliminar, in: XI Congresso Brasileiro de Meteorologia, Rio de Janeiro.

GOES-R Algorithm Working Group, 2017. GOES-R Series Product Definition and Users' Guide, 5. https://www.goes-r.gov/products/docs/PUG-L2+-vol5.pdf.

Gomes, H., Ambrizzi, T., Pontes da Silva, B., Hodges, K., Silva Dias, P., Herdies, D., Silva, M., Gomes, H., 2019. Climatology of easterly wave disturbances over the tropical South Atlantic. Clim. Dyn. 53, 1393–1411. https://doi.org/10.1007/s00382-019-04667-7.

Goodman, S., Buechler, D., Wright, P., Rust, W., 1988. Lightning and precipitation history of a microburst-producing storm. Geophys. Res. Lett. 15, 1185–1188. https://doi.org/10.1029/GL015i011p01185.

Goodman, S., Mach, D., Koshak, W., Blakeslee, R., 2012. GLM Lightning Cluster-Filter Algorithm. Algorithm Theoretical Basis Document. NOAA (Version 3.0). http://www.star.nesdis.noaa.gov/goesr/docs/ATBD/LCFA.pdf.

Goodman, S., Blakeslee, R., Koshak, W., Mach, D., Bailey, J., Buechler, D., Carey, L., Schultz, C., Bateman, M., McCaul, E., Stano, G., 2013. The GOES-R Geostationary lightning mapper (GLM). Atmos. Res. 125, 34–49. https://doi.org/10.1016/j.atmosres.2013.01.006.

Höller, H., Betz, H., Schmidt, K., Calheiros, R., May, P., Hougninou, E., Scialom, G., 2009. Lightning characteristics observed by a VLF/LF lightning detection network (LINET) in Brazil, Australia, Africa and Germany. Atmos. Chem. Phys. 9, 7795–7824. https://doi.org/10.5194/acp-9-7795-2009.

Iwabe, C., Da Rocha, R., 2009. An event of stratospheric air intrusion and its associated secondary surface cyclogenesis over the South Atlantic Ocean. J. Geophys. Res. 114 https://doi.org/10.1029/2008JD011119.

Kinzer, G., 1974. Cloud-to-ground lightning versus radar reflectivity in Oklahoma thunderstorms. J. Atmos. Sci. 31, 787–799. https://doi.org/10.1175/1520-0469(1974)031<0787:CTGLVR>2.0.CO;2.

Kitagawa, M., Brook, M., 1960. A comparison of intracloud and cloud-to-ground lightning discharges. J. Geophys. Res. 65, 1189–1201. https://doi.org/10.1029/JZ065i004p01189.

Kitagawa, N., Brook, M., Workman, E.J., 1962. Continuing currents in cloud-to-ground lightning discharges. J. Geophys. Res. 67, 637–647. https://doi.org/10.1029/JZ067i002p00637.

Kodama, Y., 1992. Large-scale common features of subtropical precipitation zones (the Baiu frontal zone, the SPCZ, and the SACZ) part I: Characteristics of subtropical frontal zones. J. Meteor. Soc. Jpn. 70, 813–836. https://doi.org/10.2151/jmsj1965.70.4_813.

Kousky, V., 1979. Frontal influences on Northeast Brazil. Mon. Weather Rev. Boston. 107, 1140–1153.

Kousky, E., 1980. Diurnal rainfall variation in Northeast Brazil. Mon. Weather Rev. 108, 488–498.

Kousky, V., Ferreira, N., 1981. Interdiurnal surface pressure variation in Brazil: their spatial distribution, origins and effects. Mon. Weather Rev. 109, 1999–2008. https://doi.org/10.1175/1520-0493(1981)109<1999:ISPVIB>2.0.CO;2.

Kousky, V., Gan, M., 1981. Upper tropospheric cyclonic vortices in the tropical South Atlantic. Tellus 33 (6), 538–551. https://doi.org/10.3402/tellusa.v33i6.10775.

Lay, E., Holzworth, R., Rodger, C., Thomas, J., Pinto Jr., O., Dowden, R., 2004. WWLL global lightning detection system: Regional validation study in Brazil. Geophys. Res. Lett. 31 https://doi.org/10.1029/2003GL018882.

Liebmann, B., Kiladis, G., Marengo, J., Ambrizzi, T., Glick, J., 1999. Submonthly convective variability over South America and the South Atlantic convergence zone. J. Clim. 12, 1877–1891. https://doi.org/10.1175/1520-0442(1999)012<1877:SCVOSA>2.0.CO;2.

Lyons, W., Bruning, E., Warner, T., MacGorman, D., Edgington, S., Tillier, C., Mlynarczyk, J., 2020. Megaflashes: just how long can a lightning discharge get? Bull. Am. Meteorol. Soc. 101, E73–E86. https://doi.org/10.1175/BAMS-D-19-0033.1.

Macgorman, D., Burgess, D., 1994. Positive cloud-to-ground lightning in tornadic storms and hailstorms. Mon. Weather Rev. 122, 1671–1697. https://doi.org/10.1175/1520-0493(1994)122<1671:PCTGLI>2.0.CO;2.

Mach, D., Christian, H., Blakeslee, R., Boccippio, D., Goodman, S., Boeck, W., 2007. Performance assessment of the optical transient detector and lightning imaging sensor. Part II: clustering algorithm. J. Geophys. Res, 112. https://doi.org/10.1029/2006JD007787.

Marengo, J., Hastenrath, S., 1993. Case studies of extreme climatic events in the Amazon basin. J. Clim. 6, 617–627. https://doi.org/10.1175/1520-0442(1993)006<0617:CSOECE>2.0.CO;2.

Matsumoto, S., Ninomiya, K., Hasegawa, R., Miki, Y., 1982. The structure and the role of a subsynoptic-scale cold vortex on the heavy precipitation. J. Meteor. Soc. Jpn. 60, 339–354. https://doi.org/10.2151/jmsj1965.60.1_339.

Morales Rodriguez, C., 2019. Thunderstorm efficiency regimes in South America as observed by STARNET and TRMM. J. Geophys. Res. 124, 11428–11451. https://doi.org/10.1029/2019JD030950.

Morales Rodriguez, C., Neves, J., Moimza, E., Roggério, V., Camara, K., Rodrigues, N., Gondim, R., Santos, F., 2015. 9 years of lightning measurements in South America as detected by STARNET. In: International Symposium on Lightning Protection (XIII SIPDA), pp. 334–336. https://doi.org/10.1109/SIPDA.2015.7339313.

Murphy, M., Said, R., 2020. Comparisons of lightning rates and properties from the US National Lightning Detection Network (NLDN) and GLD360 with GOES-16 geostationary lightning mapper and advanced baseline imager data. J. Geophys. Res. 125 https://doi.org/10.1029/2019JD031172 e2019JD031172.

Naccarato, K., Pinto, O., 2012. Lightning detection in Southeastern Brazil from the new Brazilian Total Lightning Network (BrasilDAT). In: International Conference on Lightning Protection (ICLP), Vienna, pp. 1–9. https://doi.org/10.1109/ICLP.2012.6344294.

Nascimento, E., Ambrizzi, T., 2002. The influence of atmospheric blocking on the Rossby wave propagation in Southern Hemisphere winter flows. J. Meteor. Soc. Jpn. 80, 139–159. https://doi.org/10.2151/jmsj.80.139.

Nobre, C., 1983. Tropical heat sources and their associated large-scale atmospheric circulation. In: First Conference on Southern Hemisphere Meteorology. São José dos Campos/SP, pp. 104–107.

Nogués-Paegle, J., Mo, K., 1997. Alternating wet and dry conditions over South America during summer. Mon. Weather Rev. 125, 279–291. https://doi.org/10.1175/1520-0493(1997)125<0279:AWADCO>2.0.CO;2.

Ogawa, T., 1995. Lightning currents. In: Volland, H. (Ed.), Handbook of Atmospheric Electrodynamics. CRC Press, Boca Raton, pp. 93–136.

Orville, R., Henderson, R., Bosart, L., 1983. An east coast lightning detection network. Bull. Am. Meteor. Soc. 64, 1029–1037. https://doi.org/10.1175/1520-0477(1983)064<1029:AECLDN>2.0.CO;2.

Palharini, R., Vila, D., 2017. Climatological behavior of precipitating clouds in the northeast region of Brazil. Adv. Meteorol. https://doi.org/10.1155/2017/5916150.

Peterson, M., 2020. Removing solar artifacts from Geostationary Lightning Mapper data to document lightning extremes. J. Appl. Remote. Sens. 14, 1. https://doi.org/10.1117/1.jrs.14.032402.

Peterson, M., 2021. Where are the most extraordinary lightning megaflashes in the Americas? Bull. Am. Meteorol. Soc. 102, E660–E671. https://doi.org/10.1175/BAMS-D-20-0178.1.

Peterson, M., Lang, T., Bruning, E., Albrecht, R., Blakeslee, R., Lyons, W., et al., 2020. New World Meteorological Organization certified megaflash lightning extremes for flash distance (709 km) and duration (16.73 s) recorded from space. Geophys. Res. Lett. 47 https://doi.org/10.1029/2020GL088888 e2020GL088888.

Pinto Jr., O., Pinto, I., 2000. Tempestades e Relâmpagos no Brasil. Instituto Nacional de Pesquisas Espaciais.

Quadro, M., Abreu, M., 1994. Estudos de episódios de Zonas de Convergência do Atlântico Sul sobre a América do Sul. In: Congresso Brasileiro de Meteorologia, Belo Horizonte, 8, pp. 620–623.

Raia, A., Cavalcanti, I., 2008. The life cycle of the south American monsoon system. J. Clim. 21 (23), 6227–6246. https://doi.org/10.1175/2008JCLI2249.1.

Reboita, M., Ambrizzi, T., Silva, B., Pinheiro, R., Da Rocha, R., 2019. The South Atlantic subtropical anticyclone: present and future climate. Front. Earth Sci. 7, 8. https://doi.org/10.3389/feart.2019.00008.

Reynolds, S., Brook, M., Gourley, M., 1957. Thunderstorm charge separation. J. Meteorol. 14, 426–436.

Rodrigues, M., Franco, D., Sugahara, S., 2004. Climatologia de frentes frias no litoral de Santa Catarina. Rev. Bras. Geof. 22, 135–151. https://doi.org/10.1590/S0102-261X2004000200004.

Rudlosky, S., Fuelberg, H., 2013. Documenting storm severity in the mid-Atlantic region using lightning and radar information. Mon. Weather Rev. 141, 3186–3202. https://doi.org/10.1175/MWR-D-12-00287.1.

Rudlosky, S., Virts, K., 2021. Dual geostationary lightning mapper observations. Mon. Weather Rev. 149 (4), 979–998. https://doi.org/10.1175/MWR-D-20-0242.1.

Rudlosky, S., Goodman, S., Virts, K., Bruning, E., 2019. Initial geostationary lightning mapper observations. Am. Geophys. Union 46, 1097–1104. https://doi.org/10.1029/2018GL081052.

Sacramento Neto, O., Escobar, G., Silva, P., 2010. Método objetivo para identificar episódios de Zonas de Convergência de Umidade (ZCOU) no ambiente operacional do Centro de Previsão de Tempo e Estados Climáticos-CPTEC. In: Congresso Brasileiro De Meteorologia, p. 16.

Said, R., Cohen, M., Inan, U., 2013. Highly intense lightning over the oceans: estimated peak currents from global GLD360 observations. J. Geophys. Res. 118, 6905–6915. https://doi.org/10.1002/jgrd.50508.

Salio, P., Nicolini, M., Zipser, E., 2007. Mesoscale convective systems over southeastern South America and their relationship with the South American low-level jet. Mon. Weather Rev. 135, 1290–1309. https://doi.org/10.1175/MWR3305.1.

Sant'anna Neto, J., 2006. Primeiras impressões dos cronistas e viajantes sobre o tempo e o clima no brasil colônia. Revista Bibliográfica De Geografía Y Ciencias Sociales. 11, 691.

Satyamurty, P., Mattos, L., 1989. Climatological lower tropospheric frontogeneis in the midlatitudes due to horizontal deformation and divergence. Mon. Weather Rev. 117, 1355–1364. https://doi.org/10.1175/1520-0493(1989)117<1355:CLTFIT>2.0.CO;2.

Schultz, C., Petersen, W., Carey, L.D., 2011. Lightning and severe weather: a comparison between total and cloud-to ground lightning trends. Weather Forecast. 26, 744–755. https://doi.org/10.1175/WAF-D-10-05026.1.

Seluchi, M., Marengo, J., 2000. Tropical–midlatitude exchange of air masses during summer and winter in South America: Climatic aspects and examples of intense events. Int. J. Climatol. 20, 1167–1190. https://doi.org/10.1002/1097-0088(200008)20:10<1167::AID-JOC526>3.0.CO;2-T.

Silva, W., Nascimento, M., Menezes, W., 2015. Atmospheric blocking in the South Atlantic during the summer 2014: a synoptic analysis of the phenomenon. Atmos. Clim. Sci. 5 https://doi.org/10.4236/acs.2015.54030.

Soula, S., Chauzy, S., 2001. Some aspects of the correlation between lightning and rain activities in thunderstorms. Atmos. Res. 56, 355–373. https://doi.org/10.1016/S0169-8095(00)00086-7.

Sugahara, S., Da Rocha, R., Rodrigues, M., 1994. Atmospheric conditions associated with the South America low level jet. In: Proc. Eighth Brazilian Congress of Meteorology, 2, pp. 573–577.

Tapia, A., Smith, J., Dixon, M., 1998. Estimation of convective rainfall from lightning observations. J. Appl. Meteorol. 37, 1497–1509. https://doi.org/10.1175/1520-0450(1998)037<1497:EOCRFL>2.0.CO;2.

Torres, R., Ferreira, N., 2011. Case studies of easterly wave disturbances over Northeast Brazil using the eta model. Weather Forecast. 26, 225–235. https://doi.org/10.1175/2010WAF2222425.1.

Utida, G., Cruz, F., Etourneau, J., Bouloubassi, I., Schefuß, E., Vuille, M., Novello, V., Prado, L., Sifeddine, A., Klein, V., Zular, A., Viana, J., Turcq, B., 2019. Tropical South Atlantic influence on Northeastern Brazil precipitation and ITCZ displacement during the past 2300 years. Sci. Rep. https://doi.org/10.1038/s41598-018-38003-6.

Uvo, C., Berndtsson, R., 1996. Regionalization and spatial properties of Ceará State rainfall in Northeast Brazil. J. Geophys. Res. 101, 4221–4233. https://doi.org/10.1029/95JD03235.

Virji, H., 1981. A preliminary study of summertime tropospheric circulation patterns over South America estimated from cloud winds. Mon. Weather Rev. 109, 599–610. https://doi.org/10.1175/1520-0493(1981)109<0599:APSOST>2.0.CO;2.

Williams, E., Geotis, S., Renno, N., Rutledge, S., Rasmussen, A., Rickenbach, T., 1992. A radar and electrical study of tropical "hot towers". J. Atmos. Sci. 49 (15), 1386–1395. https://doi.org/10.1175/1520-0469(1992)049<1386:ARAESO>2.0.CO;2.

Williams, E., Bolbi, B., Matlin, A., Weber, M., Hodanish, S., Sharp, D., Goodman, S., Raghavan, R., Buechler, D., 1999. The behavior of total lightning activity in severe Florida thunderstorms. Atmos. Res. 51, 245–265. https://doi.org/10.1016/S0169-8095(99)00011-3.

Williams, E., et al., 2002. Contrasting convective regimes over the Amazon: Implications for cloud electrification. J. Geophys. Res. 107, 1–19. https://doi.org/10.1029/2001JD000380.

Yamazaki, Y., Rao, V., 1977. Tropical cloudiness over the South Atlantic Ocean. J. Meteor. Soc. Jpn. Ser. II. 55, 205–207. https://doi.org/10.2151/jmsj1965.55.2_205.

Zhang, D., Cummins, K., 2020. Time evolution of satellite-based optical properties in lightning flashes, and its impact on GLM flash detection. J. Geophys. Res. 125 https://doi.org/10.1029/2019JD032024 e2019JD032024.

Zhou, J., Lau, K., 1998. Does a monsoon climate exist over South America? J. Clim. 11, 1020–1040. https://doi.org/10.1175/1520-0442(1998)011<1020:DAMCEO>2.0.CO;2.